Characterization of plasma exosomal microRNAs in responding to radiotherapy of human esophageal squamous cell carcinoma

NAN MIAO[1*], WENJIE CAI[2*], SIJIA DING[1*], YAJUAN LIU[1], WANHUA CHEN[3] and TAO SUN[1]

[1]Center for Precision Medicine, School of Medicine and School of Biomedical Sciences, Huaqiao University, Xiamen, Fujian 361021; [2]Department of Radiation Oncology; [3]Department of Clinical Laboratory, First Hospital of Quanzhou Affiliated to Fujian Medical University, Quanzhou, Fujian 362000, P.R. China

Received March 20, 2022; Accepted July 11, 2022

DOI: 10.3892/mmr.2022.12803

Abstract. Radiotherapy is one of the main treatment methods for esophageal squamous cell carcinoma (ESCC). Previous research has shown that plasma exosomal microRNAs (miRNAs) can predict therapeutic outcome. In the present study, to identify potential exosomal miRNAs that respond to radiotherapy, plasma exosomal miRNAs from ESCC patients undergoing radiotherapy were isolated and sequenced. Upregulated and downregulated miRNAs were detected from patients pre- and post-radiotherapy, and it was found that they play distinct roles in DNA damage process and endosomal mediated transport. Based on wound healing and Cell Counting Kit-8 assays in TE-1 human esophageal cancer cells, it was identified that representative miRNA *miR-652* and *miR-30a* alter migration but not proliferation. The present findings identified differentially expressed miRNAs in responding to radiotherapy, and added a reference to explore non-invasive plasma biomarkers to evaluate therapeutic effects in ESCC.

Introduction

Esophageal cancer (EC), which includes esophageal squamous cell carcinoma (ESCC) and esophageal adenocarcinoma (EAC), is the sixth most leading cause of cancer-related death worldwide (1,2). The five-year survival rate of patients with ESCC is less than 20%. In China, over 90% of EC cases are ESCC, and EC is ranked as the sixth most frequent cancer and the fourth leading cause of cancer-related death (3-5). The low survival rate is likely due to increased resistance (acquired or intrinsic) of tumor cells to chemo/radiotherapies (6,7).

Correspondence to: Dr Tao Sun, Center for Precision Medicine, School of Medicine and School of Biomedical Sciences, Huaqiao University, 668 Jimei Road, Xiamen, Fujian 361021, P.R. China
E-mail: taosun@hqu.edu.cn

*Contributed equally

Key words: exosome, miRNAs, radiotherapy, esophageal squamous cell carcinoma

Recent study suggested that microRNAs (miRNAs) can serve as biomarkers in predicting therapeutic outcomes in a variety of solid tumors, including EC (6). In the context of ESCC, studies have demonstrated that one set of miRNAs promotes the development of radio resistance, while another set of miRNAs sensitizes EC cells to radiation therapy treatments (6,8-10). Therefore, an improved understanding of these miRNAs in responding to ESCC radiotherapy remains demanding.

Exosomes are nanosized vesicles (30-150 nm diameter) that are secreted by most cells. They are enclosed by a lipid bilayer and carry various biomolecules, including proteins, glycans, lipids, metabolites, RNAs and DNAs (11). Studies have shown that miRNAs are the predominant RNA species transported by exosomes (12-15). Since exosomes can transport and transfer bioactive molecules, extensive studies have focused on their ability to regulate tumor growth and metastasis (16-19). Exosomal RNA has been demonstrated as the potential cancer biomarker by regulating the communications among different cells (12,20-22). For example, circUBE2Q2 regulates gastric cancer progression via the circUBE2Q2-miR-370-3p-STAT3 axis and promotes tumor metastasis through exosomal communications (22). Exosomal miR-1245 from colorectal cancer cells reprograms macrophages to tumor-associated macrophages (TAMs) with high transforming growth factor β (TGF-β) expression that enables tumor growth and metastasis (23). However, the roles of exosomal miRNAs in ESCC remain rudimentary (24-26). Understanding dynamic changes of exosomal miRNAs and their target genes will help improve the therapeutic outcome in patients with EC.

In the present study, the expression signature of plasma exosomal miRNAs in patients with ESCC was investigated before and after radiotherapy and differentially expressed miRNAs were identified. Target genes for up- and down-regulated miRNAs were then predicted and relevant biological pathways and potential biomarkers for ESCC responding to radiotherapy were identified. Finally, it was found that the changes of radiation-sensitized miR-652 and miR-30a can regulate cancer cell migration rates without changing proliferation *in vitro*. The present study provided a reference for future identification of potential biomarkers for cancer treatment through radiotherapy.

Materials and methods

Patients and sample selection. Plasma samples were collected from ESCC female patients with pre- and post-radiotherapy (mean age, 42; stage II; September 2020-December 2020), and were provided by the First Hospital of Quanzhou. Briefly, female patients with ESCC at stage II with the following characteristics were excluded from the present study: i) metastasis, ii) poorly controlled blood pressure, hyperlipidemia and diabetes, iii) alcohol consumption and cigarette smoking and iv) infectious diseases. One week before receiving radiotherapy, pre-radiotherapy plasma samples were collected. One week after having received 50 Gy radiation (2.0 Gy/fraction, 5 fractions/week, for 5 weeks), patient plasma samples were collected, termed as post-radiotherapy.

In the present study, 7 sets of pre- and post- radiotherapy plasma samples were obtained from 7 female ESCC patients at stage II (Table SI). For each patient, plasma samples were analyzed as a pair for pre- and post-radiotherapy. Plasma samples were used for the following experiments: i) exosome characterizations (n=1, sample no. 37892), ii) exosome miRNA sequencing (n=3, sample nos. 38380, 38632 and 38930, retained corresponding tumor tissues for H&E staining) and iii) reverse transcription-quantitative (RT-q) PCR validation for exosome miRNAs (n=3, sample nos. 38912, 38783 and 39221).

The present study was approved [approval no. (2018)101] by the Institution Ethic Issue Committee of the First Hospital of Quanzhou (Quanzhou, China). Signed informed consents were obtained from female patients with ESCC who received radiotherapy diagnosis.

Exosome isolation and RNA purification. Cleared plasma were isolated from 5 ml blood by ultracentrifugation-based assay as previously described (27). Next, exosomes were isolated from cleared plasma by SmartSEC™ HT EV Isolation System for Serum & Plasma (cat. no. SSEC096A-1; SBI, systembio.com). A total of 250-500 μl of cleared plasma were applied to each well of a filter plate, incubated and centrifuged (3,000 g for 10 min at 4˚C) to elute the first fraction. Equal volumes of SmartSEC Isolation Buffer were added and plasma samples were centrifuged (1,000 x g for 30 sec at 4˚C) again into a clean plate to elute the second fraction. Depending on the volume of sample loaded, the majority of exosomes was collected in either the first or second elution. Isolated exosomes were immediately used for experiments or stored at 4˚C. For a long-period storage, exosomes were frozen at -80˚C.

Exosomal RNAs were purified using SeraMir™ Exosome RNA Amplification kit (cat. no. RA808A-1; SBI). A total of 500 μl serum and 120 μl ExoQuick Media were combined and placed at 4˚C for 30 min. After centrifugation at 4,000 g for 2 min at 4˚C, 350 μl LYSIS Buffer was added to the exosome pellet and vortexed for 15 sec. A total of 200 μl 100% ethanol was added, samples were centrifuged at 4,000 g for 1 min at 4˚C, washed twice and were let to dry. A total of 30 μl elution buffer were added directly to the membrane in a spin column. Samples were centrifuged at 600 g for 2 min at 4˚C, and increased to 4,000 g for 1 min at 4˚C. Exosome RNAs (30-40 μl) were obtained. The quality and quantity of these RNA samples were determined by a NanoDrop spectrophotometer (ND-2000C; Thermo Fisher Scientific Inc.). Agilent RNA 6000 Nano assay (Agilent Technologies, Inc.) and agarose gel electrophoresis were used to check purity of the RNA samples.

Transmission electron microscopy (TEM), Nanoparticle tracking analysis (NTA) and western blot assay. The isolated exosomes were centrifuged using an airfuge at 30,000 g with 25 pounds per square inch for 45 min at 4˚C. Exosomes were fixed with 2.5% glutaraldehyde at 4˚C overnight. After washing, vesicles were loaded onto formvar/carbon-coated grids, negatively stained with aqueous phosphotungstic acid for 60 sec and images were captured with a transmission electron microscope (H7500, 100XCII; JEOL, Ltd.) at 80 kV.

Purified exosomes were diluted to 106-107 particles/ml in PBS for NTA using a Nanosight 300 equipped with v3.2.16 analytical software (Malvern Instruments, Inc.) (28,29). Two videos (25 sec each) were recorded for each sample and the software was used to estimate concentration and size of the particles. The recordings were performed at room temperature and were monitored manually. For analysis, the detection threshold was set to 6. Calibration was carried out using 100 nm polystyrene latex microspheres (Magsphere Inc. magsphere.com) diluted to PBS and then two videos were recorded.

Aliquots (5-10 μl) of isolated exosomes were dispensed into wells of a 96-well plate, and the assay was performed as recommended by the manufacturer instructions (Pierce BCA Protein Assay kit; cat. no. lL-61105; Thermo Fisher Scientific, Inc.). Total protein concentrations were determined using a linear standard curve established with bovine serum albumin. Because exosomes normally contain a common set of proteins, named tetraspanins, including CD81, CD63 and CD9 (29), expression of CD81, CD63 and CD9 was validated by western blot analysis. Total proteins were then separated by 12%-polyacrylamide gel electrophoresis. A total of 7.5 μl protein sample (5-25 μg proteins) was mixed with 2.5 μl 4X lithium dodecyl sulfate sample loading buffer (Invitrogen; Thermo Fisher Scientific, Inc.) and heated at 70˚C for 10 min. Samples were then loaded into pre-casted NuPAGE Novex 12% Bis-Tris 1.0 mm mini-gels (Invitrogen; Thermo Fisher Scientific, Inc.). Then, 5 μl pre-stained SDS-PAGE Standards (Bio-Rad Laboratories, Inc.) were loaded in each gel run.

Electrophoresis was performed at room temperature for ~45 min using a constant voltage (200 V) in 1X solution of NuPAGE MOPS SDS running buffer (Invitrogen; Thermo Fisher Scientific, Inc.) until the dye front reached the bottom of the 60-mm gel. After proteins were transferred to PVDF membrane, 5% skimmed milk powder was sealed at room temperature for 2 h. Then, blots were incubated overnight at 4˚C with appropriate antibodies. The following primary antibodies were used: CD9 (1:1,000; ~24 kDa; cat. no. MA5-31980), CD81 (1:1,000; ~24 kDa; cat. no. MA5-13548); CD63 (1:1,000; 40~60 kDa; cat. no. MA1-19281) and Ab specific for GAPDH (1:1,000; ~37 kDa; AB_10977387; all from Thermo Fisher Scientific, Inc.). The next day, blots were incubated with goat anti-rabbit antibody (1:5,000; cat. no. ab205718) and goat anti-mouse (1:5,000; cat. no. ab205719; both from Abcam) horseradish peroxidase-conjugated IgG for 2 h at room temperature. After washed with Tris-Tween (0.05%) buffer saline, blots were placed in a gel imager and treated with enhanced chemiluminescence (ECL; Bio-Rad Laboratories,

Inc.) super-sensitive solution for 1-3 min. The optical densities of bands were analyzed using ImageJ software 1.53 (National Institutes of Health) (30).

Hematoxylin-eosin (H&E) staining. Paraffin blocks of esophageal tumor tissues (Table SI) were cut into 4-μm thickness. Sections were deparaffinized in xylene and dehydrated in alcohol. Tissues were stained with Harris' hematoxylin solution for 6 h at 60-70˚C, and were then rinsed in tap water until the water was colorless. Next, 10% acetic acid and 85% ethanol in water were used to differentiate the tissue twice for 2 and 10 h each. After rinsing with tap water, tissues were soaked in saturated lithium carbonate solution for 12 h and then rinsed again with tap water. Finally, staining was performed with eosin Y ethanol solution for 48 h. Images were captured by a light microscope (Nikon Corporation).

MiRNA isolation, sequencing and analysis. RNAs in exosomes were isolated from three patients with pre- and post-radiotherapy (Table SI). Total RNA of each sample was used to prepare the miRNA sequencing library, which included the following steps: i) 3'-adaptor ligation, ii) 5'-adaptor ligation, iii) cDNA synthesis, iv) PCR amplification and v) size selection of ~150 bp PCR amplicons (corresponding to ~22 nt miRNAs) (Cloud-Seq Biotech, cloud-seq.com.cn). The libraries were denatured as single-stranded DNA molecules, captured on Illumina flow cells, amplified *in situ* as clusters and finally sequenced for 50 cycles on an Illumina HiSeq sequencer following the manufacturer's instructions.

Raw data was generated after sequencing, image analysis, base calling and quality filtering on Illumina sequencer. Q30 was used to perform the quality control. The adaptor sequences were trimmed and the adaptor-trimmed-reads (≥15 nt) were left by cutadapt software (v1.9.2,MIT). Trimmed reads from all samples were pooled, and miRDeep2 software (v2.0.0.5, MDC Berlin-Mitte) was used to predict novel miRNAs. The trimmed reads were aligned to the merged human pre-miRNA databases (known pre-miRNA from miRBase plus the newly predicted pre-miRNAs) using Novoalign software (v3.02.12, Novocraft Technologies Sdn Bhd) with at most one mismatch. The numbers of mature miRNA mapped tags were defined as the raw expression levels of that miRNA. The read counts were normalized by TPM (tag counts per million aligned miRNAs) approach. Differentially expressed miRNAs between two samples were filtered through Fold change and P-value.

TE-1 cell culture and miRNA mimics/inhibitor transfection. Human EC cell line TE-1, developed by the cell bank at the Chinese Academy of Science, was reported to maintain biological characteristics of ESCC (31). TE-1 cells were cultured in RPMI-1640 with 10% exosome-free fetal bovine serum (FBS, both Thermo Fisher Scientific, Inc.) and maintained in an incubator containing 5% CO_2 at 37˚C. The exosome-free FBS was produced by centrifugation (100,000 g) at 4˚C overnight in order to ensure the removal of any bovine-derived exosomes. TE-1 cells ($3x10^5$) were seeded in a six-well plate and incubated 12 h at 37˚C for attachment. Cells were then transfected at 37˚C using Lipofectamine™ 3000 (Thermo Fisher Scientific, Inc.) with mimics or inhibitors (10 μl; 20 μM) according to the manufacturer's protocol for 12, 24 and 72 h. 12, 24 and 72 h subsequent experiments were performed. Transient overexpression and inhibition of miR-30a-3p/miR-652-3p were performed by transfection with miRNA oligonucleotides (miR-30a-3p mimics, CUUUCAGUCGGAUGUUUGCAGC, miR-652-3p mimics: AAUGGCGCCACUAGGGUUGUG, miR-30a-3p inhibitors: GCUGCAAACAUCCGACUGAAAG, miR-652-3p inhibitors: CACAACCCUAGUGGCGCCAUU, mimics negative controls: AGGCAAGCUGACCCUGAAGU, inhibitor negative control: CAGUACUUUUGUGUAGUACAA, 2 OD miRNA oligonucleotides were dissolved in ddH_2O as the 20 μM solution, which were purchased from the Shanghai GenePharma Co., Ltd.).

RT-qPCR. RNAs in exosomes were isolated from three patients with pre- and post-radiotherapy (Table SI). After exosome RNA extraction (SeraMir™ Exosome RNA Amplification kit,cat. no. RA808A-1,SBI), cDNA for polyA miRNA RT-qPCR was synthesized using All-in-One miRNA First-Strand cDNA Synthesis kit (GeneCopoeia, Inc.) according to the manufacturer's protocols. Expression levels of mRNA from cells were tested using RT-qPCR with specific primers in triplicates. U6 (Rnu6-1) was used as an endogenous control for miRNA. Quantitative expression was conducted on the ABI 7500 real-time PCR system (Applied Biosystems; Thermo Fisher Scientific, Inc.). qPCR was performed using the qPCR SYBRGreen Mix (Bio-Rad Laboratories, Inc.). The relative expression levels of miRNAs were calculated using the $2^{-\Delta\Delta Cq}$ method (32). The primers for RT-qPCR are shown in Table SII.

Wound healing and Cell Counting Kit-8 (CCK-8) assay. TE-1 cells were treated with the miRNA mimics or inhibitor for 72 h. Cells were harvested and seeded in a six-well plate at a density of $2x10^5$ cells/well. When cells reached 70-80% confluence, medium was replaced with serum-free DMEM (Thermo Fisher Scientific, Inc.). A scratch wound was generated using a sterile 200-μl pipette tip, and floating cells were removed by washing with 1X PBS. Images of the scratches were captured using an inverted light microscope at x100 magnification at 0, 24 and 72 h after scratching. The wound area was normalized as follows: wound area (%)=A_n/A_0 x100, where A_0 represents the area of initial wound area in control group, A_n represents the remaining area of wound at 24 or 72 h. The data were representative of three independent experiments in triplicates. 96-well plates ($2x10^4$ TE-1 cells/well) were used here to inoculate and culture TE-1 cells at 37˚C with 5% CO_2. After being incubated for 0, 24, 48 and 72 h, 10 μl CCK-8 solution (cat. no. CK04; Dojindo Laboratories, Inc.) was added. After 2 h, the absorbance was assessed at 450 nm. The data were representative of three independent experiments in triplicate.

MiRNA target prediction and function analysis. Target prediction of miRNAs was performed using TargetScan Human7.2 (http://www.targetscan.org/vert_72/) and Funrich software 3.1.3 (http://funrich.org/) (33).

Predicted target genes were imported into the OmicShare tools, a free online platform for data analysis (https://www.omicshare.com/tools). Gene Ontology (GO; http://geneontology.org/), Kyoto Encyclopedia of Genes and Genomes

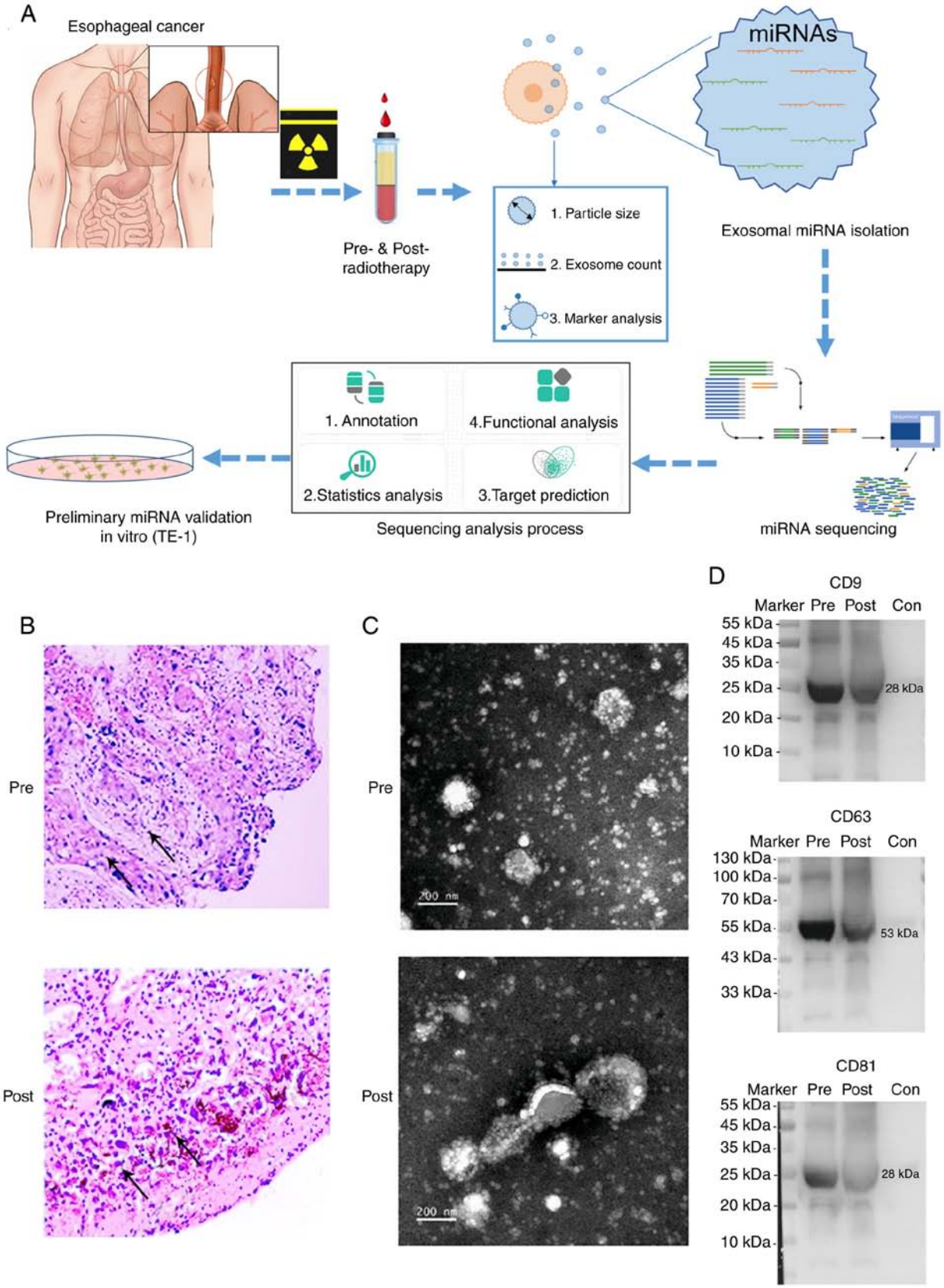

Figure 1. Exosome miRNA validation and sequencing. (A) The experimental workflow of characterization of plasma exosome miRNAs for the radiotherapy of human esophageal cancer. (B) H&E staining of esophageal squamous cell carcinoma samples (magnification, x100) from patients of pre- and post-radiotherapy. (C) Characterization of plasma exosomes. Morphological observation of exosomes by transmission electron microscopy. Scale bar=200 nm. (D) Expression levels of CD9, CD63 and CD81 were identified using western blot analysis. miRNA, microRNA.

(KEGG; https://www.kegg.jp) and Disease Ontology (DO; https://disease-ontology.org/) analysis of the miRNAs-targets with differential expression levels was performed. FunRich 3.1.3 (funrich.org/) was used to compare functional analysis,

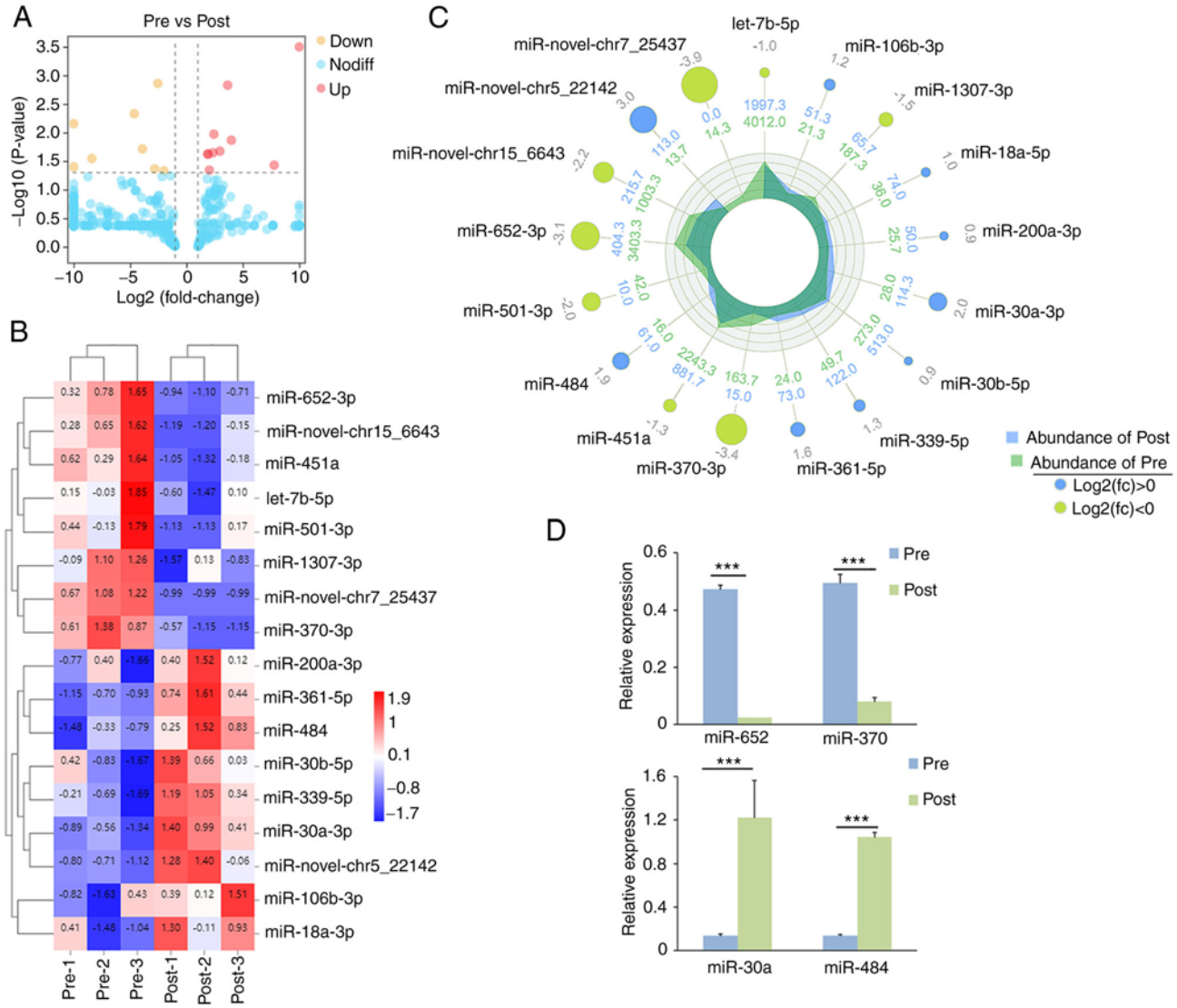

Figure 2. Differential expression of miRNAs in plasma exosomes of ESCC patients of pre- and post-radiotherapy. (A) Volcano plot of whole miRNA expression levels in Pre- and Post-groups. Each point represents a miRNA, 'yellow' dot means downregulated and 'red' dot means upregulated (pre- vs. post-miRNAs). (B) The heat map of normalized expression of miRNAs in pre- and post-radiotherapy groups. The heat map was drawn with relative expression levels of each miRNAs. Blue, white and red indicate low, middle and high expression levels of miRNAs, respectively. Color map was used to distinguish the difference of expression. Each column represents an experimental condition (such as different comparison groups or samples), and each row represents the $\log_2^{\text{Ratio-value}}$ of a gene. Different expression changes or expression amounts are illustrated in different colors. Blue, white and red indicate low, middle and high expression levels of miRNAs, respectively. (C) Radar circus of the most significantly up- and downregulated genes of pre- and post-radiotherapy groups. From outside to inside: miRNAs with $\log_2^{\text{(fold-change)}}$, miRNA expression in pre- and post-radiotherapy groups. (D) Validation of expression levels of 4 up- and downregulated miRNAs using reverse transcription-quantitative PCR in ESCC plasma exosomes. Values of histogram represent the mean ± SEM (n=3), ***P<0.001; unpaired Student's t-test). miRNA, microRNA; ESCC, esophageal squamous cell carcinoma.

clinical phenotype analysis and site of expression (33). In the present study, modules in the gene-miRNA-KEGG were mined with Cytoscape 3.9.1, and then functional enrichment analysis was applied to the miRNAs in the modules (34). Volcano map, radar map, Circular map, heatmap, Lollipop chart and Sankey diagram construction were performed using the OmicShare tools, a free online platform for data analysis (https://www.omicshare.com/tools).

Statistical analysis. The P-values were used to verify statistically significant difference and were determined by unpaired Student's t-test for assessing the significance of differences by SPSS version 25 (IBM Corp.). P<0.05 was considered to indicate a statistically significant difference.

Results

Characterizations of ESCC patient tumor samples and plasma exosomes. To explore whether exosomal miRNAs respond to radiation treatment of ESCC, plasma samples were obtained from three female ESCC patients (mean age=42; stage II, without metastasis), and exosomal miRNAs were extracted and sequenced (Fig. 1A). Patients were treated with radiotherapy (pre- and post-radiotherapy). Tumor samples from patients for ESCC plasma exosomal miRNA sequencing were stained with H&E (Table SI). Microscopy revealed an irregular cell shape, large, irregular and deeply stained nuclei, and single keratinocytes, confirming the diagnosis of squamous cell carcinoma (Fig. 1B) (35). Following radiotherapy,

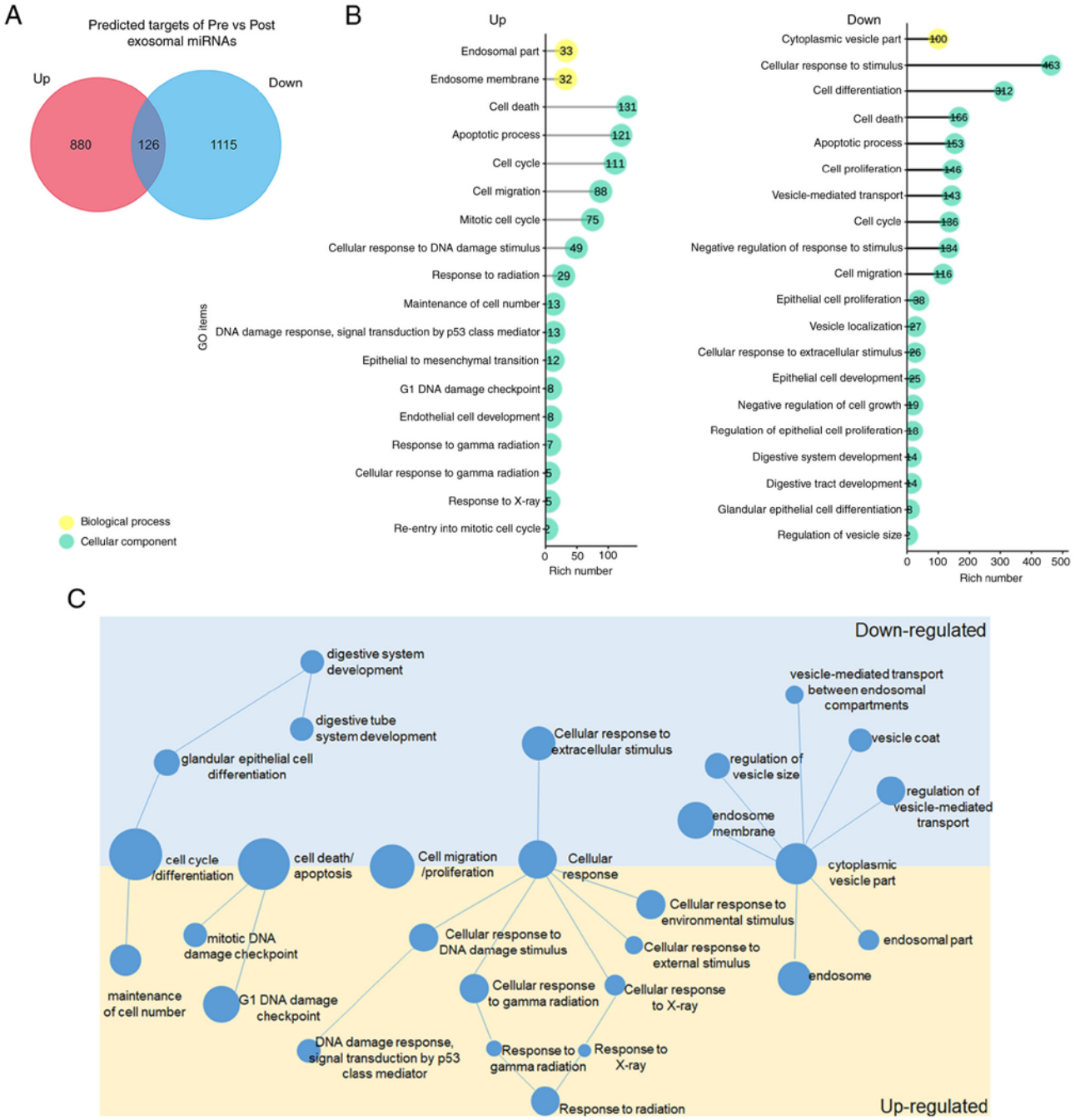

Figure 3. Target prediction and GO analysis in up- and downregulated miRNAs in pre- vs. post-radiotherapy groups. (A) Venn diagrams of the target genes for up- and downregulated miRNAs. (B) Lollipop of target genes for up- and downregulated miRNAs in GO analysis. The yellow circle represents the cellular component, and the green circle represents the biological process. (C) The comparison network of GO items of up- and downregulated miRNAs. The yellow background represents the items enriched in upregulated targets, and the blue background represents the items enriched in downregulated targets. miRNA, microRNA; GO, Gene Ontology.

tumor cells with calcifications, larger and blurred nuclei, apoptosis and necrosis were detected (Fig. 1B). These changes revealed the typical radiological indicator of early cancers (stage I-II; Fig. 1B) (35).

Exosomes were isolated from pre- and post-radiotherapy plasma samples of 7 patients with ESCC (Fig. 1C). Isolated exosomes were characterized by TEM. Sizes of exosomes in pre- and post- groups were 68.28±19.07 and 77.47±26.87 nm, and exosomal concentrations of two groups were $2.12x10^{10}$ and $2.22x10^{10}$ particles/ml, respectively (Table SIII and Fig. S1). High resolution TEM examinations further showed cup-shaped vesicles of extracted exosomes (Fig. 1C). Moreover, expression of three established exosome markers, such as CD63, CD9 and CD81 were readily identified using western blot analysis (Fig. 1D) (29,36,37). These results indicated that exosomes with a high quality are extracted from the plasma of ESCC patients with pre- and post-radiotherapy.

Differential expression of miRNAs in exosomes of plasma samples of pre- and post-radiotherapy. To determine whether profiles of exosomal miRNAs from pre- and post-radiotherapy

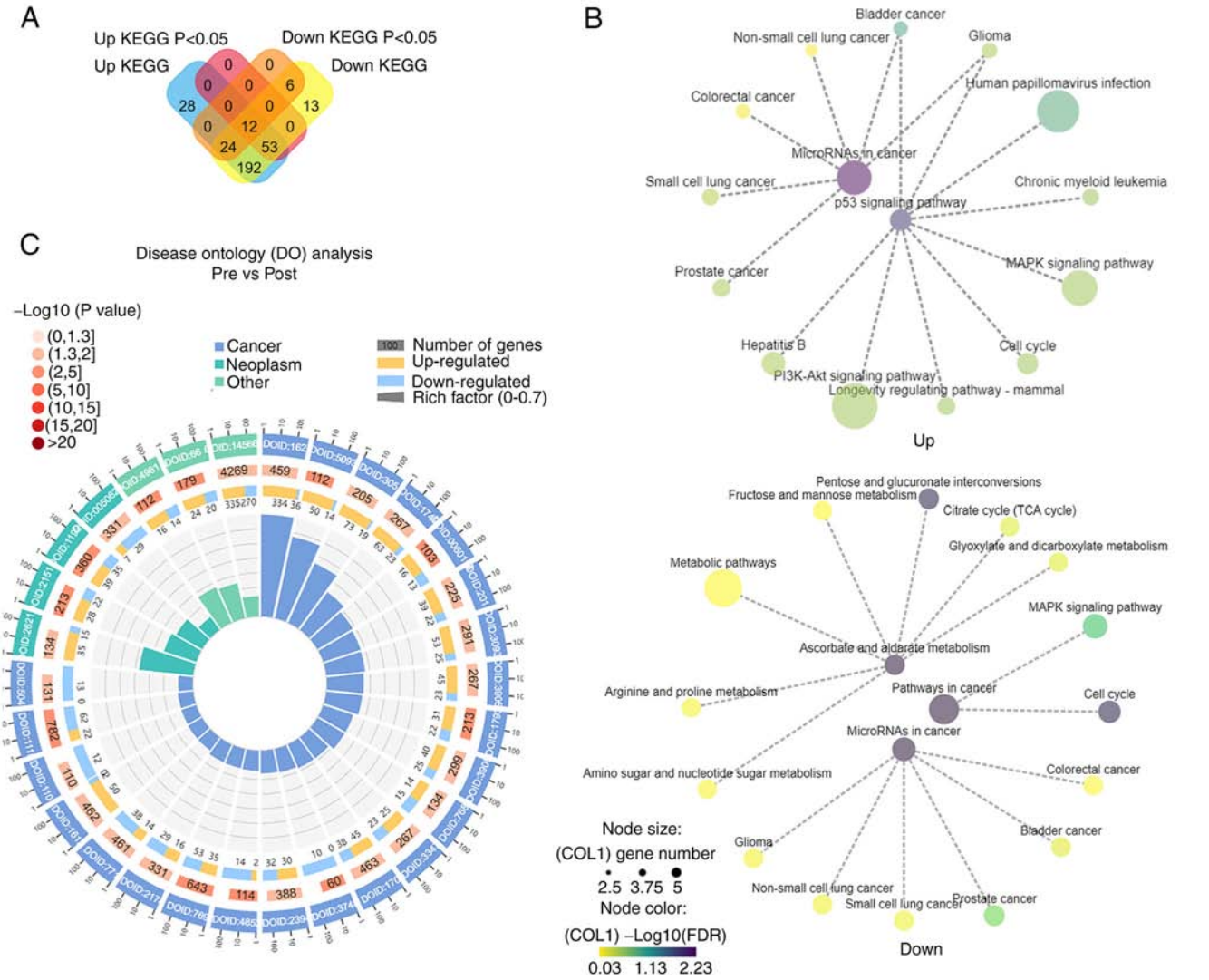

Figure 4. KEGG and DO analysis in up- and downregulated miRNAs. (A) Venn diagrams of the enriched KEGG pathways for the targets of up- and downregulated miRNAs. (B) The networks of target genes for downregulated vs. upregulated miRNAs in signal pathways. The colors from yellow, green to purple represent the values of $-\log_{10}^{(FDR)}$, and the node sizes represent the gene numbers. (C) Comparison analysis of DO analysis in miRNAs of pre-and post-radiotherapy. Classified as 3 functions: Cancer, neoplasm and other diseases. From outside to inside: i) enrichment classification, outside the circle is the coordinate ruler of gene numbers. Different colors represent different categories; ii) P-values of this classification in background genes. The more genes, the longer the bars, the smaller the values, the redder the color is; iii) bar chart of upregulated gene proportion, dark purple represents upregulated gene proportion, light purple represents downregulated gene proportion; iv) Rich Factor value of each classification (the number of foreground genes in this classification divided by the number of background genes), and each small bar of background auxiliary line represents 0.1. KEGG, Kyoto Encyclopedia of Genes and Genomes; DO, Disease Ontology.

plasma samples may differ, total RNAs were isolated from exosomes, and small RNA libraries were prepared for miRNA sequencing and annotation (Fig. 1A).

Combining 3 samples from pre- and post-radiotherapy groups and removing low signals, 726 miRNAs were obtained (Table SIV). A total of 8 miRNAs highly expressed in the pre-radiotherapy group (fold-change (pre-/post-)>1, $\log_2^{\text{fold-change}}>0$ and P<0.05) and 9 miRNAs highly expressed in the post-radiotherapy group were detected (Fig. 2A and B and Table SV). The upregulated (fold-change (pre-/post-)>1, $\log_2^{\text{fold-change}}>0$, P<0.05) and downregulated (fold-change (Pre-/Post-)<1, $\log_2^{\text{fold-change}}<0$, P<0.05) miRNAs with the mean expression and fold-changes were shown in a Radar graph (Fig. 2C). Certain well-studied miRNAs such as miR-106b, miR-18a, miR-200a, miR-30a/b, let-7b and miR-370 exhibited differential expression, and certain new miRNAs (miR-novel-chr5_22142, miR-novel-chr15_6643 and miR-novel-chr7_25437) were detected as well. The sequencing results were further verified using RT-qPCR. As examples, among tested miRNAs, transcriptional levels of the upregulated (miR-652 and miR-370) and downregulated (miR-30a and miR-484) miRNAs were consistent with the exosomal sequencing results (Fig. 2D). These results suggested that plasma exosomal miRNAs are sensitive and responding to the radiotherapy of ESCC.

Target prediction and GO analysis of up- and downregulated miRNAs. Since miRNAs normally function through silencing their target genes, predicted targets of differentially expressed exosomal miRNAs were next searched. A total of 1,106 genes were predicted as targets of upregulated miRNAs, 1,241 genes as targets of downregulated miRNAs

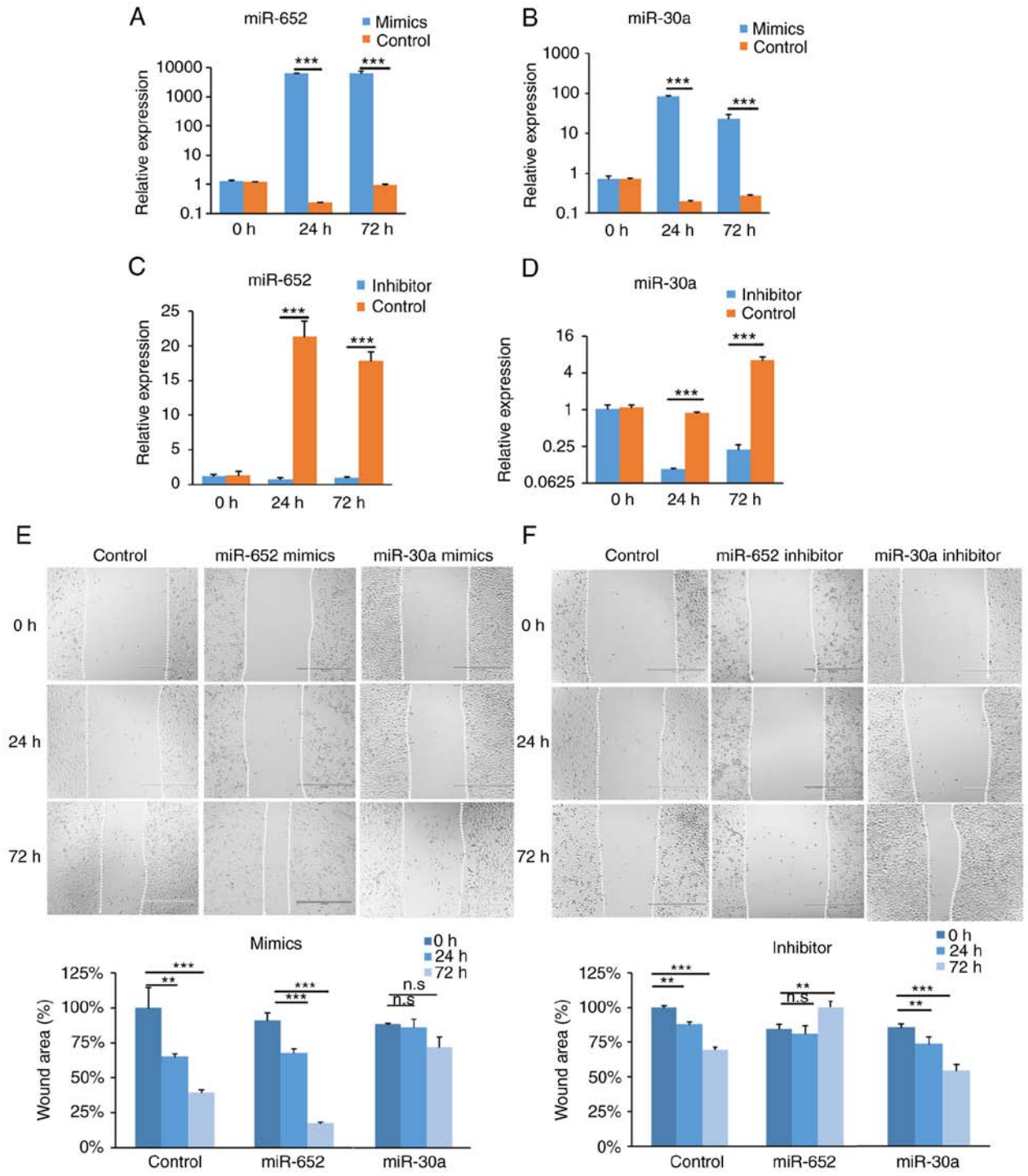

Figure 5. Cell migration analyses of miR-652 and miR-30a in TE-1 cells. (A and B) Relative expression levels of (A) miR-652 and (B) miR-30a in control and mimics groups. (C and D) Relative expression levels of (C) miR-652 and (D) miR-30a in control and inhibitor groups. (E) Normalized cell scratched result of miR-652 and miR-30a after 0, 24 and 72 h in control and mimics groups. (F) Normalized cell scratched result of miR-652 and miR-30a after 0, 24 and 72 h in control and overexpression groups. The cell scratched size was normalized in 0 h of the control group as the 100% (n=3). **P<0.01 and ***P<0.001 (unpaired Student's t-test). miR, microRNA.

and 126 genes were overlapped in two groups using TargetScan Human7.2 and Funrich software 3.1.3 (Fig. 3A; Tables SVI and SVII).

Functions of predicted targets of up- and downregulated miRNAs were next analyzed by GO analysis, and abundant items in Biological Process, Cellular Component and Molecular Function were identified (P<0.05; Figs. S2 and S3; Tables SVIII and SIX). It was found that targets of both up- and downregulated miRNAs play a role in cell cycle/differentiation, cell death/apoptosis, cell migration/proliferation, cellular response and cytoplasmic vesicle part (Fig. 3B and C). Moreover, targets of upregulated miRNAs were abundant in maintenance of cell number, DNA damage process, multiple cellular response, endosome and endosome part, while targets of downregulated miRNAs were involved in vesicle part, glandular epithelial cell differentiation and digestive system

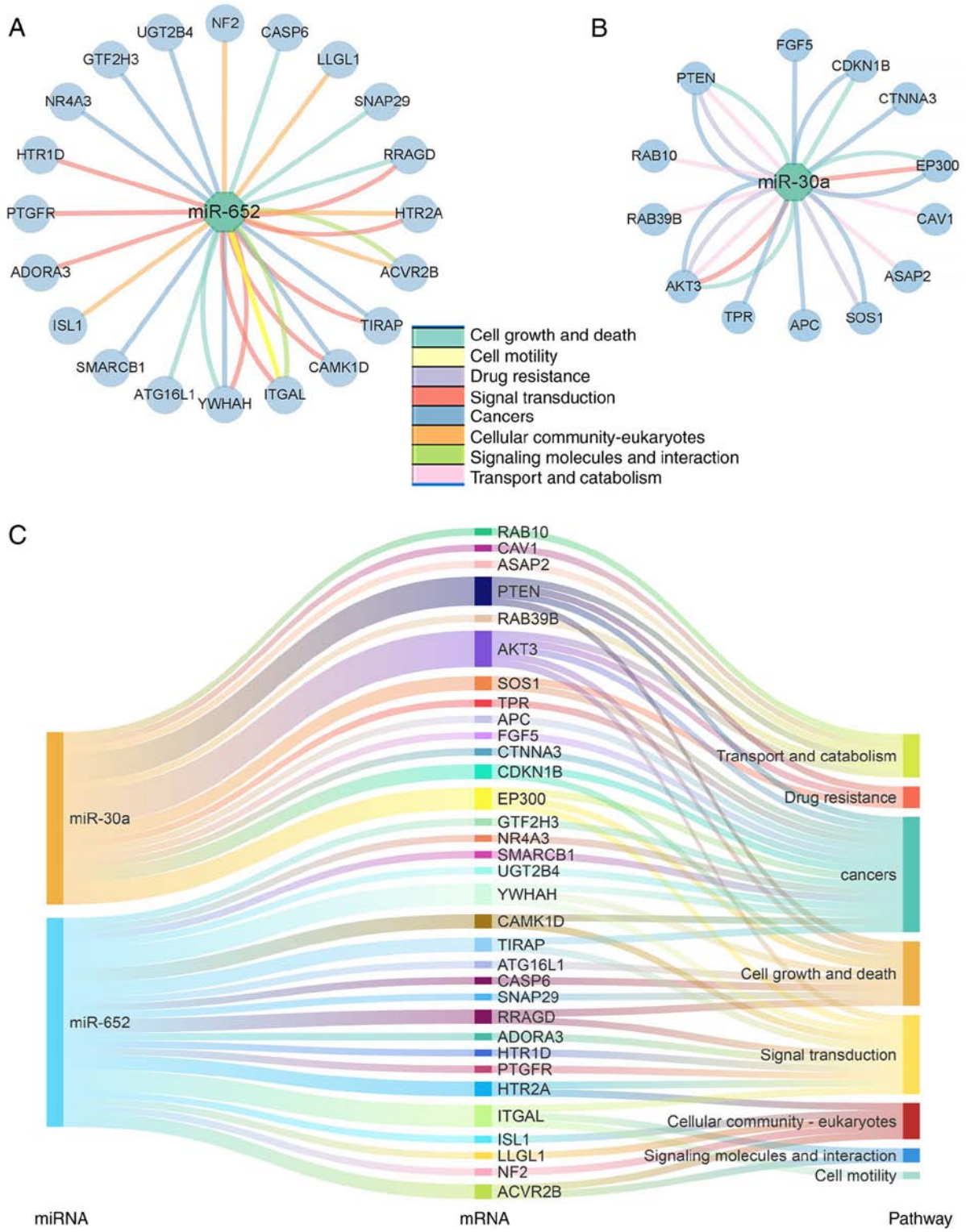

Figure 6. Target analysis of miR-652 and miR-30a. (A) Target analysis network of miR-652. (B) Target analysis network of miR-30a. Colors of lines represent different classifications, from top to bottom: cell growth and death, cell motility, drug resistance, signal transduction, cancers, cellular community-eukaryotes, signaling molecules and interaction and transport and catabolism. (C) Sankey map of target genes of miR-30a and miR-652 in different pathways. miR, microRNA.

development (Fig. 3B and C). These results suggested the distinct functions of targets of up- and downregulated plasma exosomal miRNAs.

KEGG and DO analysis. Interactions between up- and downregulated miRNAs and their predicted targets were next studied using KEGG analyses (Figs. 4 and S4; Tables SX and SXI). Based on the Venn graph, 65 of 309 pathways were significantly abundant ($P<0.05$) in upregulated miRNA targets, 42 of 300 pathways were significantly abundant ($P<0.05$) in downregulated miRNA targets, and 12 pathways were overlapped in two groups (Fig. 4A).

Based on the KEGG correlation network, it was found that top 15 pathways of targets of downregulated miRNAs play a role in multiple cancer processes, such as prostate and lung cancer, and the p53 signaling pathway. Top 15 pathways of targets of downregulated miRNAs function in pathways associated with cancer such as cell cycle and the MAPK signaling pathway, and ascorbate and aldarate metabolism (Fig. 4B). These KEGG analyses suggested that altered miRNAs of pre- and post-radiotherapy may function in different pathways.

Interactions between miRNAs and their predicted targets were next investigated using DO analysis. The targets of upregulated miRNAs were enriched in digestive system cancers such as pancreas adenocarcinoma, pancreatic ductal adenocarcinoma and pancreatic carcinoma (Figs. 4C and S5; Table SXII). The targets of downregulated miRNAs were enriched in central nervous system cancer such as cerebral ventricle cancer, cerebrum cancer, synovial sarcoma, malignant glioma, brain cancer and atypical teratoid rhabdoid tumor (Figs. 4C and S5; Table SXIII). These results suggested the up- and downregulated plasma exosomal miRNAs play different roles in cancer processes.

Cell migration and proliferation analyses of miR-652 and miR-30a in TE-1 cells. Our miRNA sequencing and RT-qPCR results showed that miR-652 and miR-30a are sensitive and responding to the radiotherapy of ESCC. Previous studies have shown that miR-652 inhibits proliferation and invasion of ESCC by targeting FGFR1 and other genes, and miR-30a may negatively regulates FoxD1 in ESCC (38-41). Thus, miR-652 and miR-30a were selected and their roles in migration in TE-1 cells, a human EC cell line, were examined using wound-healing assays (31,42,43) (Fig. 1A).

The expression of miR-652 and miR-30a was altered by overexpressing and knocking down in TE-1 cells (31). Wound-healings were detected at 0, 24 and 72 h after scratching (Fig. 5). Compared with those at 0 h, the normalized wound sizes of the miR-652 overexpression group (miRNA mimics) were significantly decreased by 23.28% at 24 h, and by 73.54% at 72 h (Fig. 5A and E). Conversely, the normalized wound sizes of the miRNA inhibitor group were significantly increased by 15.42% at 72 h (Fig. 5C and F). Moreover, to investigate the miRNA effect in proliferation, a CCK-8 assay was performed in TE-1 cells, which is widely used to examine cell growth or proliferation (44,45). Proliferation of TE-1 cells was not significantly changed by miR-652 overexpression and inhibition (Fig. S6A and B). These results suggested that altering miR-652 expression affects TE-1 cell migration but not proliferation.

The potential role of miR-30a in migration and proliferation (Fig. 5) was next examined. Compared with the control group, the normalized wound sizes of the miR-30a mimics group showed no change (Fig. 5B and E). Conversely, the normalized wound sizes of the inhibitor group were significantly decreased by 11.50% at 24 h and by 29.94% at 72 h (Fig. 5D and F). Proliferation of TE-1 cells was not significantly changed by miR-30a overexpression and inhibition (Fig. S6C and D). These results indicated that inhibition of miR-30a directly prevents cancer cell migration *in vitro*.

Potential roles of target genes of miR-652 and miR-30a. It was found that the radiotherapy sensitive miR-652 and miR-30a may play roles in migration of TE-1 cells. Target genes of miR-652 and miR-30a were next analyzed using the KEGG analysis. A total of 8 different molecular processes of their targets including cell growth and death, cell motility, drug resistance, signal transduction, cancers, cellular community-eukaryotes, signaling molecules and interaction and transport and catabolism were chosen (Fig. 6). Among these targets, 20 target genes of miR-652 and 13 target genes of miR-30a were enriched in the 8 aforementioned molecular processes (Fig. 6A and B).

To visualize the potential role of predicted targets, Sankey diagrams were constructed to illustrate a relationship of genes, pathways and miRNAs (Fig. 6C). Certain previously demonstrated target-miRNA pairs such as *PTEN-miR30a*, *AKT3-miR30a*, *EP300-miR652*, *YWHAH-miR652* and *ITGAL-miR652* were readily detected (Fig. 6C). These gene-miRNA pairs may play an essential role in responding to radiotherapy in ESCC.

Discussion

Radiotherapy is a major therapeutic way for ESCC (46-48). Studies have shown that miRNAs derived from plasma exosomes can be used to evaluate the curative effect of radiotherapy (49-51). Previous studies have shown that some specific miRNAs are sensitized by radiotherapy in ESCC (52,53). In the present study, to identify exosomal miRNAs that may be responding to radiotherapy in non-metastatic ESCC, differentially expressed exosomal miRNAs were analyzed in plasma samples of patients with pre- and post-radiotherapy using miRNA sequencing and RT-qPCR. It was identified that upregulated miRNAs play specific roles in responding to radiation and DNA damage, and downregulated miRNAs play roles in exosome transduction. Among them, upregulated miR-652 and downregulated miR-30a directly altered migration but not proliferation of human EC cells *in vitro*. The present study indicated that certain exosomal miRNAs are responding to radiotherapy in ESCC patients, and provided new plasma biomarkers for future evaluation of diagnosis, treatment and prognosis of ESCC.

Accumulating studies have shown that circulating exosomes are associated with cancer progression and therapeutic reactions, for instance in ESSC (54-57). Moreover, radiation exposure increases the levels of intracellular free radical species, followed by DNA strand breaks and subsequent dysfunction of the mitochondria, endoplasmic reticulum and other organelles (58). These radiation-induced cellular events lead to activation of pro-apoptotic signaling and eventually to tumor cell killing (59). Thus, the present study aimed to identify miRNAs in exosomes that may be responding to radiotherapy in ESSC. A total of 8 and 9 miRNAs with up- and downregulated expression in pre- and post-radiotherapy plasma samples were identified, respectively. Certain identified miRNAs in the present study have also been shown as novel circulating factors in responding to radiotherapy in other types of cancer (52,53,60-62). Moreover, a higher level of plasma miR-339-5p, which was also identified in the present study, has been shown to be associated with radiotherapy sensitivity and

favorable survival by targeting *Cdc25A* gene in ESCC (53). Therefore, radiotherapy causes significant alterations in expression levels of exosomal miRNAs in ESCC plasma.

Furthermore, because miRNAs normally negatively regulate expression levels of target genes, it was revealed that targets of upregulated exosomal miRNAs are enriched in DNA damage check point and cellular response to radiation, while targets of downregulated miRNAs are enriched in endosome transport and digestive system development. For instance, target genes for upregulated miRNAs after radiotherapy are involved in the p53 signaling pathway and are enriched in digestive system cancers based on the present study. These results suggested that radiation sensitive miRNAs in plasma exosomes may be developed into non-invasive biomarkers for evaluating the radiation-induced esophageal toxicity and therapeutic effect in the future (63). More specimen and detailed target examinations are required to uncover biomarkers of miRNA-target pairs in the future studies.

Among identified exosomal miRNAs in the present study, miR-652 and miR-30a have been demonstrated to regulate cell migration in cancers of the digestive system by other laboratories (64-67). It appears that miR-652 directly inhibits tumor invasion by targeting *FGFR1*, *PLD1* and other genes (38,39). The present study also showed the effect of miR-652 and miR-30a on cell migration but not proliferation in TE-1 cells, an EC cell line. Moreover, our miRNA-target pair analyses indicated that targets for miR-652 and miR-30a are enriched in multiple biological and cellular processes, which may correlate with cancer cell migration and invasion. In addition, it is likely that miR-652 and miR-30a play a general role in cancer development. Studies have shown that miR-652 executes a tumor-promoter function in non-small cell lung cancer through direct binding and regulating the expression of *Lgl1* (68), and miR-30a plays a central role in regulating the PTEN/AKT pathway in lung adenocarcinoma and liver cancer cells (69,70). The present findings provided a reference for further identification of miRNA-target interaction networks in responding to radiotherapy of ESCC. The future studies will be to validate miRNA-target regulations and to examine the biological meanings of these interactions.

In summary, certain exosomal miRNAs sensitive to radiotherapy were identified in the present study, which may be developed into biomarkers for evaluation of the effect of radiotherapy for human ESCC. Identifying and validating interactions of miRNAs and their targets in responding to radiotherapy will help us to design radiotherapy strategies in an improved way and optimize treatment effects in the future.

Acknowledgements

Not applicable.

Funding

The present study was supported by the Fundamental Research Funds for the Central Universities (grant no. ZQN-1020), the Scientific Research Funds of Huaqiao University (grant nos. 16BS815, 19BS303 and Z16Y0017), the Natural Science Foundation of Fujian, China (grant nos. 2019J01071 and 605-52519051), the Innovation Awards of Quanzhou Talents (grant no. 2018C057R), Quanzhou City Science & Technology Program of China (grant no. 2018C057R) and the National Natural Science Foundation of China (grant nos. 31771141 and 32100775).

Availability of data and materials

All data generated or analyzed during this study are included in this published article.

Authors' contributions

TS conceived and designed the experiments. WCa and SD performed sample collection. NM, SD, WCh and WCa conducted RNA extraction and analysis of results. NM, WCh and YL performed bioinformatics analysis. NM and TS wrote and edited the manuscript. NM and TS confirm the authenticity of all the raw data. All authors have read and approved the final manuscript.

Ethics approval and consent to participate

The present study was approved [approval no. (2018)101] by the Institution Ethic Issue Committee of the First Hospital of Quanzhou (Quanzhou, China). Signed informed consents were obtained from female patients with ESCC who received radiotherapy diagnosis.

Patient consent for publication

Not applicable.

Competing interests

The authors declare that they have no competing interests.

References

1. Kelsen D: Principles and practice of gastrointestinal oncology. Lippincott, Williams & Wilkins, Philadelphia, PA, 2008.
2. Jemal A, Bray F, Center MM, Ferlay J, Ward E and Forman D: Global cancer statistics. CA Cancer J Clin 61: 69-90, 2011.
3. Lin Y, Totsuka Y, He Y, Kikuchi S, Qiao Y, Ueda J, Wei W, Inoue M and Tanaka H: Epidemiology of esophageal cancer in Japan and China. J Epidemiol 23: 233-242, 2013.
4. Zheng RS, Sun KX, Zhang SW, Zeng HM, Zou XN, Chen R, Gu XY, Wei WW and He J: Report of cancer epidemiology in China, 2015. Zhonghua Zhong Liu Za Zhi 41: 19-28, 2019 (In Chinese).
5. He Z and Ke Y: Precision screening for esophageal squamous cell carcinoma in China. Chin J Cancer Res 32: 673-682, 2020.
6. Malhotra A, Sharma U, Puhan S, Bandari NC, Kharb A, Arifa PP, Thakur L, Prakash H, Vasquez KM and Jain A: Stabilization of miRNAs in esophageal cancer contributes to radioresistance and limits efficacy of therapy. Biochimie 156: 148-157, 2019.
7. Klug F, Prakash H, Huber PE, Seibel T, Bender N, Halama N, Pfirschke C, Voss RH, Timke C, Umansky L, *et al*: Low-dose irradiation programs macrophage differentiation to an iNOS(+)/M1 phenotype that orchestrates effective T cell immunotherapy. Cancer Cell 24: 589-602, 2013.
8. Liu J, Xue N, Guo Y, Niu K, Gao L, Zhang S, Gu H, Wang X, Zhao D and Fan R: CircRNA_100367 regulated the radiation sensitivity of esophageal squamous cell carcinomas through miR-217/Wnt3 pathway. Aging (Albany NY) 11: 12412-12427, 2019.
9. Zhang YH, Wang QQ, Li H, Ye T, Gao F and Liu YC: miR-124 radiosensitizes human esophageal cancer cell TE-1 by targeting CDK4. Genet Mol Res 15: 15027893, 2016.

10. Chen Z, Hu X, Wu Y, Cong L, He X, Lu J, Feng J and Liu D: Long non-coding RNA XIST promotes the development of esophageal cancer by sponging miR-494 to regulate CDK6 expression. Biomed Pharmacother 109: 2228-2236, 2019.
11. Mathieu M, Martin-Jaular L, Lavieu G and Thery C: Specificities of secretion and uptake of exosomes and other extracellular vesicles for cell-to-cell communication. Nat Cell Biol 21: 9-17, 2019.
12. Wei Z, Batagov AO, Schinelli S, Wang J, Wang Y, Fatimy RE, Rabinovsky R, Balaj L, Chen CC, Hochberg F, *et al*: Coding and noncoding landscape of extracellular RNA released by human glioma stem cells. Nat Commun 8: 1145, 2017.
13. Zhang H, Freitas D, Kim HS, Fabijanic K, Li Z, Chen H, Mark MT, Molina H, Martin AB, Bojmar L, *et al*: Identification of distinct nanoparticles and subsets of extracellular vesicles by asymmetric flow field-flow fractionation. Nat Cell Biol 20: 332-343, 2018.
14. Balandeh E, Mohammadshafie K, Mahmoudi Y, Pourhanifeh MH, Rajabi A, Bahabadi ZR, Mohammadi AH, Rahimian N, Hamblin MR and Mirzaei H: Roles of non-coding RNAs and angiogenesis in glioblastoma. Front Cell Dev Biol 9: 716462, 2021.
15. Zhang J, Li S, Li L, Guo C, Yao J and Mi S: Exosome and exosomal microRNA: Trafficking, sorting, and function. Genomics Proteomics Bioinformatics 13: 17-24, 2015.
16. Costa-Silva B, Aiello NM, Ocean AJ, Singh S, Zhang H, Thakur BK, Becker A, Hoshino A, Mark MT, Molina H, *et al*: Pancreatic cancer exosomes initiate pre-metastatic niche formation in the liver. Nat Cell Biol 17: 816-826, 2015.
17. Peinado H, ković MA, Lavotshkin S, Matei I, Costa-Silva B, Moreno-Bueno G, Hergueta-Redondo M, Williams C, García-Santos G, Ghajar CM, *et al*: Corrigendum: Melanoma exosomes educate bone marrow progenitor cells toward a pro-metastatic phenotype through MET. Nat Med 22: 1502, 2016.
18. Peinado H, Aleckovic M, Lavotshkin S, Matei I, Costa-Silva B, Moreno-Bueno G, Hergueta-Redondo M, Williams C, García-Santos G, Ghajar C, *et al*: Melanoma exosomes educate bone marrow progenitor cells toward a pro-metastatic phenotype through MET. Nat Med 18: 883-891, 2012.
19. Hoshino A, Costa-Silva B, Shen TL, Rodrigues G, Hashimoto A, Mark MT, Molina H, Kohsaka S, Giannatale AD, Ceder S, *et al*: Tumour exosome integrins determine organotropic metastasis. Nature 527: 329-335, 2015.
20. Skog J, Wurdinger T, van Rijn S, Meijer DH, Gainche L, Sena-Esteves M, Curry WT Jr, Carter BS, Krichevsky AM and Breakefield XO: Glioblastoma microvesicles transport RNA and proteins that promote tumour growth and provide diagnostic biomarkers. Nat Cell Biol 10: 1470-1476, 2008.
21. Valadi H, Ekstrom K, Bossios A, Sjöstrand M, Lee JJ and Lötvall JO: Exosome-mediated transfer of mRNAs and microRNAs is a novel mechanism of genetic exchange between cells. Nat Cell Biol 9: 654-659, 2007.
22. Yang J, Zhang X, Cao J, Xu P, Chen Z, Wang S, Li B, Zhang L, Xie L, Fang L and Xu Z: Circular RNA UBE2Q2 promotes malignant progression of gastric cancer by regulating signal transducer and activator of transcription 3-mediated autophagy and glycolysis. Cell Death Dis 12: 910, 2021.
23. Cooks T, Pateras IS, Jenkins LM, Patel KM, Robles AI, Morris J, Forshew T, Appella E, Gorgoulis VG and Harris CC: Mutant p53 cancers reprogram macrophages to tumor supporting macrophages via exosomal miR-1246. Nat Commun 9: 771, 2018.
24. Chen F, Chu L, Li J, Shi Y, Xu B, Gu J, Yao X, Tian M, Yang X and Sun X: Hypoxia induced changes in miRNAs and their target mRNAs in extracellular vesicles of esophageal squamous cancer cells. Thorac Cancer 11: 570-580, 2020.
25. Chen F, Xu B, Li J, Yang X, Gu J, Yao X and Sun X: Hypoxic tumour cell-derived exosomal miR-340-5p promotes radioresistance of oesophageal squamous cell carcinoma via KLF10. J Exp Clin Cancer Res 40: 38, 2021.
26. Butz F, Eichelmann AK, Mayne GC, Wang T, Bastian I, Chiam K, Marri S, Sykes PJ, Wijnhoven BP, Toxopeus E, *et al*: MicroRNA profiling in oesophageal adenocarcinoma cell lines and patient serum samples reveals a role for miR-451a in radiation resistance. Int J Mol Sci 21: 8898, 2020.
27. Zheng Y, Campbell EC, Lucocq J, Riches A and Powis SJ: Monitoring the Rab27 associated exosome pathway using nanoparticle tracking analysis. Exp Cell Res 319: 1706-1713, 2013.
28. Zhang W, Peng P, Kuang Y, Yang J, Cao D, You Y and Shen K: Characterization of exosomes derived from ovarian cancer cells and normal ovarian epithelial cells by nanoparticle tracking analysis. Tumour Biol 37: 4213-4221, 2016.
29. Simpson RJ, Jensen SS and Lim JW: Proteomic profiling of exosomes: Current perspectives. Proteomics 8: 4083-4099, 2008.
30. Schneider CA, Rasband WS and Eliceiri KW: NIH image to imageJ: 25 years of image analysis. Nat Methods 9: 671-675, 2012.
31. Li BQ XJ, Li QZ, Li XY, Gu FZ and Mu XL: A study on cell biological characters of human esophageal cancer cell line TE-1. Chin J Mod Med 13: 33-35, 2011 (In Chinese).
32. Livak KJ and Schmittgen TD: Analysis of relative gene expression data using real-time quantitative PCR and the 2(-Delta Delta C(T)) method. Methods 25: 402-408, 2001.
33. Fonseka P, Pathan M, Chitti SV, Kang T and Mathivanan S: FunRich enables enrichment analysis of OMICs datasets. J Mol Biol 433: 166747, 2021.
34. Otasek D, Morris JH, Boucas J, Pico AR and Demchak B: Cytoscape automation: Empowering workflow-based network analysis. Genome Biol 20: 185, 2019.
35. Feng H, Hu YY, Jin P, Meng XK, Chen YB and Zhang HM: Intensity-modulated radiotherapy combined with iodine-125 seed implantation in non-central recurrence of cervical cancer: A case report and literature review. Oncol Letters 14: 4085-4091, 2017.
36. Jeppesen DK, Fenix AM, Franklin JL, Higginbotham JN, Zhang Q, Zimmerman LJ, Liebler DC, Ping J, Liu Q, Evans R, *et al*: Reassessment of exosome composition. Cell 177: 428-445.e18, 2019.
37. Kowal J, Arras G, Colombo M, Jouve M, Morath JP, Primdal-Bengtson B, Dingli F, Loew D, Tkach M and Théry C: Proteomic comparison defines novel markers to characterize heterogeneous populations of extracellular vesicle subtypes. Proc Natl Acad Sci USA 113: E968-E977, 2016.
38. Lu M, Song Y, Fu W, Liu Y, Huai S, Cui X, Pang L, Yang L and Wei Y: MicroRNA and target mRNA selection through invasion and cytotoxicity cell modeling and bioinformatics approaches in esophageal squamous cell carcinoma. Oncol Rep 38: 1181-1189, 2017.
39. Zhen C, Huang J and Lu J: MicroRNA-652 inhibits the biological characteristics of esophageal squamous cell carcinoma by directly targeting fibroblast growth factor receptor 1. Exp Ther Med 18: 4473-4480, 2019.
40. Yan Q, Liu L, Yang H, Xu C, Wang Z, Wang Q, Wu Z, Wu C, Dong L, Wang J and Wu M: Long non-coding RNA OIP5-AS1 inhibits the proliferation and migration of esophageal squamous carcinoma cells by targeting FOXD1/miR-30a-5p axis and the effect of micro- and nano-particles on targeting transfection system. J Biomed Nanotechnol 17: 1380-1391, 2021.
41. Wada M, Goto Y, Tanaka T, Okada R, Moriya S, Idichi T, Noda M, Sasaki K, Kita Y, Kurahara H, *et al*: RNA sequencing-based microRNA expression signature in esophageal squamous cell carcinoma: oncogenic targets by antitumor miR-143-5p and miR-143-3p regulation. J Hum Genet 65: 1019-1034, 2020.
42. Duff D and Long A: Roles for RACK1 in cancer cell migration and invasion. Cell Signal 35: 250-255, 2017.
43. Rodriguez LG, Wu X and Guan JL: Wound-healing assay. Methods Mol Biol 294: 23-29, 2005.
44. Wang F, Chen TS, Xing D, Wang JJ and Wu YX: Measuring dynamics of caspase-3 activity in living cells using FRET technique during apoptosis induced by high fluence low-power laser irradiation. Lasers Surg Med 36: 2-7, 2005.
45. Morita Y, Naka T, Kawazoe Y, Fujimoto M, Narazaki M, Nakagawa R, Fukuyama H, Nagata S and Kishimoto T: Signals transducers and activators of transcription (STAT)-induced STAT inhibitor-1 (SSI-1)/suppressor of cytokine signaling-1 (SOCS-1) suppresses tumor necrosis factor alpha-induced cell death in fibroblasts. Proc Natl Acad Sci USA 97: 5405-5410, 2000.
46. Chan WWL, Lam KO and Kwong DLW: Radiotherapy for thoracic esophageal squamous cell carcinoma. Methods Mol Biol 2129: 307-319, 2020.
47. Zou B, Tu Y, Liao D, Xu Y, Wang J, Huang M, Ren L, Zhu J, Gong Y, Liu Y, *et al*: Radical esophagectomy for stage II and III thoracic esophageal squamous cell carcinoma followed by adjuvant radiotherapy with or without chemotherapy: Which is more beneficial? Thorac Cancer 11: 631-639, 2020.
48. Deng W, Yang J, Ni W, Li C, Chang X, Han W, Zhou Z, Chen D, Feng Q, Liang J, *et al*: Postoperative radiotherapy in pathological T2-3N0M0 thoracic esophageal squamous cell carcinoma: Interim report of a prospective, phase III, randomized controlled study. Oncologist 25: e701-e708, 2020.
49. Al-Mayah AH, Irons SL, Pink RC, Carter DR and Kadhim MA: Possible role of exosomes containing RNA in mediating nontargeted effect of ionizing radiation. Radiat Res 177: 539-545, 2012.

50. Su LL, Chang XJ, Zhou HD, Hou LB and Xue XY: Exosomes in esophageal cancer: A review on tumorigenesis, diagnosis and therapeutic potential. World J Clin Cases 7: 908-916, 2019.
51. Jin X, Chen Y, Chen H, Fei S, Chen D, Cai X, Liu L, Lin B, Su H, Zhao L, *et al*: Evaluation of tumor-derived exosomal miRNA as potential diagnostic biomarkers for early-stage non-small cell lung cancer using next-generation sequencing. Clin Cancer Res 23: 5311-5319, 2017.
52. Luo A, Zhou X, Shi X, Zhao Y, Men Y, Chang X, Chen H, Ding F, Li Y, Su D, *et al*: Exosome-derived miR-339-5p mediates radiosensitivity by targeting Cdc25A in locally advanced esophageal squamous cell carcinoma. Oncogene 38: 4990-5006, 2019.
53. Sun Y, Wang J, Ma Y, Li J, Sun X, Zhao X, Shi X, Hu Y, Qu F and Zhang X: Radiation induces NORAD expression to promote ESCC radiotherapy resistance via EEPD1/ATR/Chk1 signalling and by inhibiting pri-miR-199a1 processing and the exosomal transfer of miR-199a-5p. J Exp Clin Cancer Res 40: 306, 2021.
54. Zhu L, Zhao L, Wang Q, Zhong S, Guo X, Zhu Y, Bao J, Xu K and Liu S: Circulating exosomal miRNAs and cancer early diagnosis. Clin Transl Oncol 24: 393-406, 2021.
55. Lv J, Zhao HP, Dai K, Cheng Y, Zhang J and Guo L: Circulating exosomal miRNAs as potential biomarkers for Barrett's esophagus and esophageal adenocarcinoma. World J Gastroenterol 26: 2889-2901, 2020.
56. Avgeris M, Panoutsopoulou K, Papadimitriou MA and Scorilas A: Circulating exosomal miRNAs: Clinical significance in human cancers. Expert Rev Mol Diagn 19: 979-995, 2019.
57. Schwarzenbach H: The clinical relevance of circulating, exosomal miRNAs as biomarkers for cancer. Expert Rev Mol Diagn 15: 1159-1169, 2015.
58. Skladanowski A, Bozko P and Sabisz M: DNA structure and integrity checkpoints during the cell cycle and their role in drug targeting and sensitivity of tumor cells to anticancer treatment. Chem Rev 109: 2951-2973, 2009.
59. Koukourakis MI: Radiation damage and radioprotectants: New concepts in the era of molecular medicine. Brit J Radiol 85: 313-330, 2012.
60. Li MH, Zou X, Xia T, Wang T, Liu P, Zhou X, Wang S and Zhu W: A five-miRNA panel in plasma was identified for breast cancer diagnosis. Cancer Med 8: 7006-7017, 2019.
61. Tang Y, Cui Y, Li Z, Jiao Z, Zhang Y, He Y, Chen G, Zhou Q, Wang W, Zhou X, *et al*: Radiation-induced miR-208a increases the proliferation and radioresistance by targeting p21 in human lung cancer cells. J Exp Clin Canc Res 35: 7, 2016.
62. Ham IH, Lee D and Hur H: Cancer-associated fibroblast-induced resistance to chemotherapy and radiotherapy in gastrointestinal cancers. Cancers (Basel) 13: 1172, 2021.
63. Xu T, Liao ZX, O'Reilly MS, Levy LB, Welsh JW, Wang LE, Lin SH, Komaki R, Liu Z, Wei Q and Gomez DR: Serum inflammatory miRNAs predict radiation esophagitis in patients receiving definitive radiochemotherapy for non-small cell lung cancer. Radiother Oncol 113: 379-384, 2014.
64. Zhang J, Qiu WQ, Zhu H, Liu H, Sun JH, Chen Y, Shen H, Qian CL and Shen ZY: HOTAIR contributes to the carcinogenesis of gastric cancer via modulating cellular and exosomal miRNAs level. Cell Death Dis 11: 780, 2020.
65. Yao W, Guo P, Mu Q and Wang Y: Exosome-derived Circ-PVT1 contributes to cisplatin resistance by regulating autophagy, invasion, and apoptosis via miR-30a-5p/YAP1 axis in gastric cancer cells. Cancer Biother Radiopharm 36: 347-359, 2021.
66. Kulkarni B, Gondaliya P, Kirave P, Rawal R, Jain A, Garg R and Kalia K: Exosome-mediated delivery of miR-30a sensitize cisplatin-resistant variant of oral squamous carcinoma cells via modulating Beclin1 and Bcl2. Oncotarget 11: 1832-1845, 2020.
67. Gao P, Wang D, Liu M, Chen S, Yang Z, Zhang J, Wang H, Niu Y, Wang W, Yang J and Sun G: DNA methylation-mediated repression of exosomal miR-652-5p expression promotes oesophageal squamous cell carcinoma aggressiveness by targeting PARG and VEGF pathways. PLoS Genet 16: e1008592, 2020.
68. Yang WH, Zhou CC, Luo M, Shi X, Li Y, Sun Z, Zhou F, Chen Z and He J: MiR-652-3p is upregulated in non-small cell lung cancer and promotes proliferation and metastasis by directly targeting Lgl1. Oncotarget 7: 16703-16715, 2016.
69. Li WF, Dai H, Ou Q, Zuo GQ and Liu CA: Overexpression of microRNA-30a-5p inhibits liver cancer cell proliferation and induces apoptosis by targeting MTDH/PTEN/AKT pathway. Tumor Biol 37: 5885-5895, 2016.
70. Sui J, Yang RS, Xu SY, Zhang YQ, Li CY, Yang S, Yin LH, Pu YP and Liang GY: Comprehensive analysis of aberrantly expressed microRNA profiles reveals potential biomarkers of human lung adenocarcinoma progression. Oncol Rep 38: 2453-2463, 2017.